THE UNIVERSITY OF
WARWICK

**Original citation:**
Stanway, Elizabeth R., Bunker, A. J., Glazebrook, K., Abraham, R. G., Rhoads, J., Malhotra, S., Crampton, D., Colless, M. and Chiu, K.. (2007) The GLARE Survey - II. Faint z 6 Ly line emitters in the HUDF. Monthly Notices of the Royal Astronomical Society, Volume 376 (Number 2). pp. 727-738. ISSN 0035-8711

**Permanent WRAP url:**
http://wrap.warwick.ac.uk/62206

warwick**publications**wrap

highlight your research

**http://wrap.warwick.ac.uk/**

# The GLARE Survey – II. Faint $z \approx 6$ Ly$\alpha$ line emitters in the HUDF

Elizabeth R. Stanway,[1]⋆† Andrew J. Bunker,[2,3] Karl Glazebrook,[4]
Roberto G. Abraham,[5] James Rhoads,[6] Sangeeta Malhotra,[6] David Crampton,[7]
Matthew Colless[8] and Kuenley Chiu[3,4]

[1]*Astronomy Department, University of Wisconsin-Madison, Sterling Hall, Madison, WI 53726, USA*
[2]*Institute of Astronomy, Madingley Road, Cambridge CB3 OHA*
[3]*School of Physics, University of Exeter, Stocker Road, Exeter EX4 4QL*
[4]*Department of Physics and Astronomy, John Hopkins University, 3400 N Charles Street, Baltimore, MD 21218, USA*
[5]*Department of Astronomy & Astrophysics, University of Toronto, 60 St George Street, Toronto, ON, Canada M5S 3H8*
[6]*Arizona State University, Department of Physics & Astronomy, Box 871504, Temp, AZ 85287, USA*
[7]*Dominion Astrophysical Observatory, 5071 W Saanich Road, Victoria, Canada V9E 2E7*
[8]*Anglo-Australian Observatory, PO Box 296, Epping, NSW 1710, Australia*

**ABSTRACT**

The galaxy population at $z \approx 6$ has been the subject of intense study in recent years, culminating in the *Hubble Ultra Deep Field* (HUDF) – the deepest imaging survey yet. A large number of high-redshift galaxy candidates have been identified within the HUDF, but until now analysis of their properties has been hampered by the difficulty of obtaining spectroscopic redshifts for these faint galaxies. Our 'Gemini Lyman-Alpha at Reionization Era' (GLARE) project has been designed to undertake spectroscopic follow-up of faint ($z' < 28.5$) $i'$-drop galaxies at $z \approx 6$ in the HUDF. In a previous paper we presented preliminary results from the first 7.5 h of data from GLARE. In this paper we detail the complete survey. We have now obtained 36 h of spectroscopy on a single GMOS slitmask from Gemini-South, with a spectral resolution of $\lambda/\Delta\lambda_{\mathrm{FWHM}} \approx 1000$. We identify five strong Ly$\alpha$ emitters at $z > 5.5$, and a further nine possible line emitters with detections at lower significance. We also place tight constraints on the equivalent width of Ly$\alpha$ emission for a further ten $i'$-drop galaxies and examine the equivalent width distribution of this faint spectroscopic sample of $z \approx 6$ galaxies. We find that the fraction of galaxies with little or no emission is similar to that at $z \approx 3$, but that the $z \approx 6$ population has a tail of sources with high rest-frame equivalent widths. Possible explanations for this effect include a tendency towards stronger line emission in faint sources, which may arise from extreme youth or low metallicity in the Lyman-break population at high redshift, or possibly a top-heavy initial mass function.

**Key words:** galaxies: evolution – galaxies: high-redshift – galaxies: starburst.

## 1 INTRODUCTION

The *Hubble Ultra Deep Field* (HUDF; Beckwith et al. 2006) opened a new window on the early universe. The exceptionally deep, multiwavelength data provided opportunities to study colour-selected samples of high-redshift galaxy candidates with modest luminosities more typical of the general galaxy population. Previously, only the most luminous 'tip of the iceberg' had been accessible. By pushing to redshifts around 6 with the $z'$-band filter and the $i'$-drop Lyman-break selection technique (e.g. Bunker et al. 2004), the HUDF explored the end of the reionization epoch signalled

by the Gunn–Peterson HI absorption trough in QSOs (Becker et al. 2001).

None the less, the use of the Lyman-break colour selection criterion to isolate star-forming galaxies at a specific redshift, first developed to study $z \approx 3$ galaxies (Steidel, Pettini & Hamilton 1995) and extended to $z \approx 6$ candidates in analysis of the Great Observatories Origins Deep Survey (GOODS) and HUDF fields (e.g. Stanway, Bunker & McMahon 2003; Bouwens et al. 2006), presents challenges. Before the properties of the population can be meaningfully discussed, the selection function itself must be understood. Estimates must be obtained of the contaminant fraction and the redshift distribution of $i'$-drop galaxies.

Many colour-selected galaxies are significantly fainter than the conventional spectroscopic limit of today's large telescopes. The

⋆E-mail: E.R.Stanway@bristol.ac.uk
†Present address: H H Wills Physics Laboratory, Bristol BS8 1TL.

HUDF reaches limits of $z'_{AB} = 28.5$ ($10\sigma$) – a depth that, until *JWST* becomes available, requires unreasonable exposure times to obtain a high signal-to-noise ratio (S/N) spectrum for the continuum. However, line emission (e.g. Ly$\alpha$) may be within reach of ultradeep moderate-dispersion spectroscopy on 8–10 m telescopes even for the faintest galaxies, provided the equivalent width of the line is large enough. If the properties of the star-forming population at $z \approx 6$ are similar to those of the Lyman-break galaxy (LBG) population at $z \approx 3$ (Steidel et al. 2003), then half the sources are expected to show the resonant Ly$\alpha$ transition in emission. Detection of a Ly$\alpha$ emission line fixes the redshift of a source, while detection or constraints on nearby high-ionization emission lines can quantify contribution by an active galactic nucleus (AGN). Furthermore, spectroscopy can enable the identification of lower redshift contaminants in the sample which will not emit Ly$\alpha$ photons at these wavelengths, but may show other emission lines. When a population of Ly$\alpha$ emitters is studied, the distribution of equivalent widths is sensitive to the stellar initial mass function (IMF) (since the Ly$\alpha$ transition is excited by emission from hot, massive, short-lived stars), and also to the fraction of neutral gas in the intergalactic medium (IGM) and the emergent photon fraction (Malhotra & Rhoads 2004).

In this paper we present results from the Gemini Lyman-Alpha at Reionization Era (GLARE) project. This programme used the 8-m Gemini-South telescope to obtain extremely deep spectroscopy on a single slitmask, centred on the HUDF (Fig. 1). By obtaining extremely long exposures using a telescope with a large collecting area, we aimed to study continuum-selected galaxies fainter than those targeted by any other survey, and to quantify the line emission properties of our $i'$-drop sample in the HUDF. We presented initial results from this programme in Stanway et al. (2004b, hereafter Paper I), which was based on 7.5 h of on-source exposure taken at low spectral resolution ($\lambda/\Delta\lambda \approx 500$). In this paper we present an analysis of the 24 $i'$-drop selected $5.6 < z < 7.0$ candidates targeted for 36 h of spectroscopy at higher resolving power ($\lambda/\Delta\lambda \approx 1200$). In Section 2 we describe the GLARE programme, and in Section 3 we present the results of our observing campaign. In Section 4 we analyse the equivalent width distribution of the GLARE line emitters, and in Section 5 we discuss the implications of this distribution in the context of other work in this field. Finally, in Section 6 we present our conclusions.
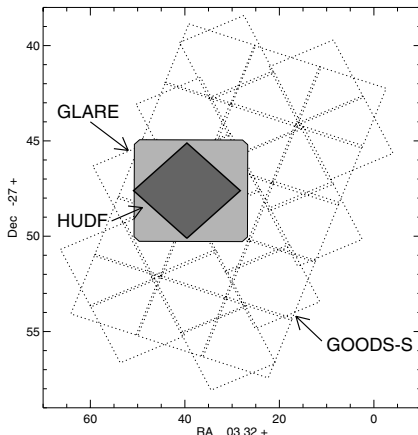


**Figure 1.** The geometry of the UDF and GOODS-S fields (taken at two position angles), and the layout of the GLARE mask. GLARE encompasses the entire UDF field, and some parts of the GOODS-S field.

We adopt the following cosmology: a flat Universe with $\Omega_\Lambda = 0.7$, $\Omega_M = 0.3$ and $H_0 = 70\,h_{70}$ km s$^{-1}$ Mpc$^{-1}$. All magnitudes are quoted in the AB system (Oke & Gunn 1983).

## 2 THE GLARE PROJECT

### 2.1 Candidate selection

The objectives of the GLARE project were to determine the redshift and line emission properties of our targets, reaching low equivalent width limits on Ly$\alpha$ emission for a uniformly selected sample of $i'$-drop LBGs (Stanway et al. 2003; Bouwens et al. 2004; Bunker et al. 2004). The $i'$-drop colour selection is sensitive to galaxies at $5.6 < z < 7.0$, although the selection sensitivity falls off rapidly above $z \approx 6.5$ (see Stanway et al. 2003). With this data we aim to probe galaxies at the end of the epoch of reionization, and compare their properties to comparable galaxy samples at lower redshift, in order to explore possible evolution in the nature of the star-forming galaxy population.

Initial results obtained from this survey were reported in Stanway et al. (2004), which presented 7.5 h spectra of three Ly$\alpha$ line emitters observed on the 2003 GLARE slitmask. Selection of targets for our 2003 observations was made possible by the early release of a list of red sources in the HUDF, based on observations to one third of its final depth, and supplemented by $i'$-drop galaxies selected from the shallower, but wider field, GOODS survey of the same region (Stanway 2004).

Between observations of our 2003 GLARE mask, and the start of semester 2004B, the full HUDF data were made public and the GLARE slitmask was redesigned accordingly. Sources with $(i' - z')_{AB} \geqslant 1.3$ and $z'_{AB} \leqslant 28.5$ in the HUDF imaging (i.e. the catalogue of Bunker et al. 2004) were assigned the highest priority for spectroscopic follow-up and 15 such sources were placed on the slitmask. The agreement is excellent between the HUDF $i'$-drop discovery catalogue of (Bunker et al. 2004), which we use as our GLARE source list, and the recent data paper by the HUDF team (Beckwith et al. 2006). All the robust $i'$-drops targeted on the GLARE slitmask are are also identified by Beckwith et al. (2006).

In order to maximize use of the mask, additional objects were targeted. Seven slits were placed on candidates (including the two emitters identified in Paper I, GLARE 3001 and 3011) from a brighter selection with $(i' - z')_{AB} \geqslant 1.3$ and $z'_{AB} \leqslant 27.5$, selected from the GOODS imaging (Stanway 2004), primarily at the edges of the slitmask and lying outside the HUDF region. A further three slits were placed on candidates with colours lying marginally outside of our GOODS selection criteria, either in colour (i.e. $1.0 < i' - z' < 1.3$) or magnitude (i.e. $z' > 27.5$), or in noisy regions of the GOODS images, and two slits on sources from the original UDF early release list of red sources that did not meet our final criteria. Two slits were placed on $z \approx 5$ $v$-band dropout candidates, and two on known low-redshift [O II] 3727 Å emitters, previously observed by VLT/FORS2 (Vanzella et al. 2006) and used as a check on flux calibration. Finally, five slits were placed on alignment stars to ensure accurate positioning of the mask, and six slits were used to conduct a blank sky survey for serendipitous sources. The composition of the 2004 GLARE slitmask is summarized in Table 1.

Both the $z'_{AB} = 27.5$ cut applied in the GOODS data and the $z'_{AB} = 28.5$ cut applied in the HUDF correspond to a signal to noise of approximately 8. We chose to work well above the detection limit in order to have confidence in the reality and nature of our candidate sources (many of which are detected only in this one band). In the event of non-detection in the $i'$ band we use the limiting magnitudes

**Table 1.** The composition of the 2004 GLARE slitmask. 1XXX indicates a GLARE identifier number in the range 1000–1999, etc.

| ID | No of slits | Description |
|---|---|---|
| 1XXX | 15 | HUDF, $i' - z' \geqslant 1.3$, $z' \leqslant 28.5$ |
| | 2 | HUDF, other red sources |
| 2XXX | 5 | Alignment stars |
| 3XXX | 7 | GOODS $i' - z' \geqslant 1.3$, $z' \leqslant 27.5$ |
| 4XXX | 2 | GOODS $v - i'$ selected, $z = 5$ cands |
| 5XXX | 2 | Known, low z, [O II] emitters |
| 6XXX | 6 | Blanks sky slits |
| 7XXX | 3 | GOODS marginal $i'$-drop candidates |
| | 42 | Total number of slits on mask |

$i'_{AB} = 29.15$ (GOODS) and $i'_{AB} = 30.4$ (HUDF) corresponding to $3\sigma$ variation in the sky background, as measured on the images. All sources were required to be undetected in the available $b$ (F435W) imaging but faint detections in the deep $v$ (F606W) filter (which lies above the Lyman limit at $z \approx 6$, and which is present in several spectroscopically confirmed $z > 5.6$ galaxies) were permitted. Completely unresolved sources were omitted from the selection although at faint magnitudes, the dividing line between unresolved and slightly resolved sources becomes blurred.

Of the line emitter candidates presented in Section 3, only GLARE 1042 and GLARE 1040 lie within the NICMOS HUDF field (Thompson et al. 2005). Both have near-infrared colours consistent with a high-redshift interpretation, as indeed did all the $i'$-drop sources in this field discussed by Stanway, McMahon & Bunker (2005).

## 2.2 Observations and data analysis

The 2004 GLARE slitmask was observed in semester 2004B using the GMOS spectrograph on Gemini-South (Hook et al. 2003). This mask was observed at higher spectral resolution than the 2003 GLARE mask, using the GMOS-S R600 grating rather than the R150, blazed at an angle of 48°.5 giving a central wavelength of ~8700 Å. As the CCD oversampled the typical seeing and spectral resolution, the image was binned at $2 \times 2$ pixel so as to reduce the readout noise and improve the S/N. After this binning, the spectral scale was 0.94 Å pixel$^{-1}$, and 0.146 arcsec pixel$^{-1}$ spatially on the detector. The slit width was 1.0 arcsec, which produced a spectral resolution of 6.5 Å FWHM for objects which fill the slit. Both mask and slits were oriented due north. The higher spectral resolution of the 2004 GLARE mask ($\lambda/\Delta\lambda \approx 1200$ compared with 500 for 2003 GLARE) decreases the fraction of the wavelength range adversely affected by OH sky lines, and also enables us to better study the profiles of emission lines from the targets. The OG515 filter was used to suppress second order light from shorter wavelengths. In order to fill CCD chip gaps and ensure full wavelength coverage in the range $\lambda \approx 7000$–$10\,000$ Å three different central wavelength settings were observed (8580, 8700 and 8820 Å). The shortest wavelength reached was 6420 Å, while the longest wavelength surveyed was 10 950 Å.

Wavelengths were calibrated from the night sky lines in each slit, leading to a solution with an rms error of approximately 0.3 Å. Fluxes were calibrated from the broadband magnitudes of the alignment stars on the mask, and checked against both line emission of known [O II] emitters also observed in VLT/FORS2 spectroscopy that had been placed on our mask for verification purposes, and ex-

isting spectroscopy for the known $z = 5.83$ Lyα emitter GLARE 1042 (Dickinson et al. 2004; Stanway et al. 2004a,b). We estimate a 20 per cent error on the flux calibration, associated with slit losses and centroiding uncertainty in the narrow slits.

To optimize the subtraction of night sky emission lines (which occupy a large fraction of the spectrum at >8000 Å) we used the instrument in 'nod and shuffle' mode (Glazebrook & Bland-Hawthorn 2001; Abraham et al. 2004). Each exposure was 30 min long, nodding every 60 s. Hence we are able to suppress sky emission that varies on time-scales longer than 1 min. The total exposure time on this mask was 36 h.

The reduction of 'nod and shuffle' data involves the subtraction of positive and negative spectra, observed in alternate 60-s exposures and offset spatially by the telescope nodding. We employed slits 2.47 arcsec in length, nodding by 1.25 arcsec between subexposures. Our queue scheduled observations were constrained by the requirement that the seeing was less than 0.5 arcsec FWHM, and the nod distance set such that the signals were separated by at least twice the seeing disc. Hence the characteristic signal of an emission line comprises a 'dipole' signal of positive and negative emission at the same wavelength, spatially offset by 1.25 arcsec. In visually identifying candidate line emitters, we looked for this dipole signature with positive and negative channels of comparable strengths; this requirement effectively increases the sensitivity of the spectroscopy beyond the formal limit, since random background fluctuations are unlikely to produce simultaneous signals in both positive and negative channels.

Dipole signals lying under strong emission sky lines are treated with caution; as well as having more Poisson noise, sky line variability and charge diffusion at the red end of the spectrum may lead to a spurious signal.

A number of charge traps and CCD artefacts were also masked when the individual exposures were combined. These charge traps affect some regions of the CCD more severely than others, and so the noise properties vary from slitlet to slitlet, and also with wavelength. However, the $1\sigma$ rms pixel-to-pixel variation in the background at 8500 Å was $1.4 \times 10^{-19}$ erg cm$^{-2}$ s$^{-1}$ Å$^{-1}$ for the $2 \times 2$ binned pixels, measured between skylines on the 'nod and shuffle' background-subtracted spectra. Hence, our sensitivity to an emission line extending over 500 km s$^{-1}$ × 1 arcsec is $2.5 \times 10^{-18}$ erg cm$^{-2}$ s$^{-1}$ ($3\sigma$ combining both nod positions, or $2\sigma$ per nod channel).

## 3 LINE EMITTERS IN THE 2004 GLARE MASK

In the 36 h exposure of the 2004 GLARE mask, we identify five strong Lyα emission line sources (including the three candidates tentatively proposed in Stanway et al. 2004b). We identify a further four sources which have lower significance detections, but which are considered possibly to be real emission lines due to their dipole natures and separation from possible sky line residuals. Finally, we identify five sources with tentative emission line detections that are considered unlikely to be real.

### 3.1 Strong emission lines

Table 2 lists the properties of the five $z \approx 6$ sources with strong Lyα line emission. Fig. 2 presents the two-dimensional spectra obtained for these sources, and the summed flux from positive and negative spectral channels. We also placed two known lower redshift galaxies on the 2004 GLARE mask, placing [O II] within our spectral range, as a check on our sensitivity and calibration. These

**Table 2.** Strong line emitters on the 2004 GLARE mask. Errors on line fluxes and equivalent widths are approximately 20 per cent. Equivalent widths are calculated from broadband magnitudes, accounting for line contamination and Ly$\alpha$ forest blanketing. $2\sigma$ limits on magnitudes are given where appropriate. Alternate ID is taken from Bunker et al. (2004). Note that GLARE 1042 lies in the chip gap of one of the three wavelength settings observed, and hence in a region with slightly lower S/N.

| ID | RA and Dec. J(2000) | Alternate ID | $z$ | $z'_{AB}$ | $i' - z'$ | Line flux (erg cm$^{-2}$ s$^{-1}$) | $W_{\mathrm{Ly}\alpha}^{\mathrm{rest}}$ (Å) | $L_{\mathrm{Ly}\alpha}$ ($10^{42}$ erg s$^{-1}$) |
|---|---|---|---|---|---|---|---|---|
| 1042[a] | 03 32 40.01 −27 48 14.9 | 20104 | 5.83 | $25.35 \pm 0.02$ | $1.64 \pm 0.04$ | $1.58 \times 10^{-17}$ | 22.9 | 5.90 |
| 1054 | 03 32 33.20 −27 46 43.3 | 42414 | 5.93 | $27.65 \pm 0.07$ | $1.45 \pm 0.17$ | $0.68 \times 10^{-17}$ | 120 | 2.63 |
| 1008 | 03 32 47.97 −27 47 05.1 | | 6.13 | $28.51 \pm 0.18$ | $>1.35$ | $0.43 \times 10^{-17}$ | 159 | 1.80 |
| 3001 | 03 32 46.04 −27 49 29.7 | | 5.79 | $26.69 \pm 0.06$ | $1.67 \pm 0.20$ | $0.77 \times 10^{-17}$ | 44.1 | 2.83 |
| 3011 | 03 32 43.18 −27 45 17.6 | | 5.93 | $27.47 \pm 0.12$ | $1.86 \pm 0.50$ | $1.13 \times 10^{-17}$ | 242 | 4.39 |

[a]GLARE 1042 has a panoply of alternate names. It is SBM03#3 in Stanway et al. (2003), 20104 in (Bunker et al. 2004) and is SiD0002, the $z = 5.83$ line emitter of Dickinson et al. (2004).
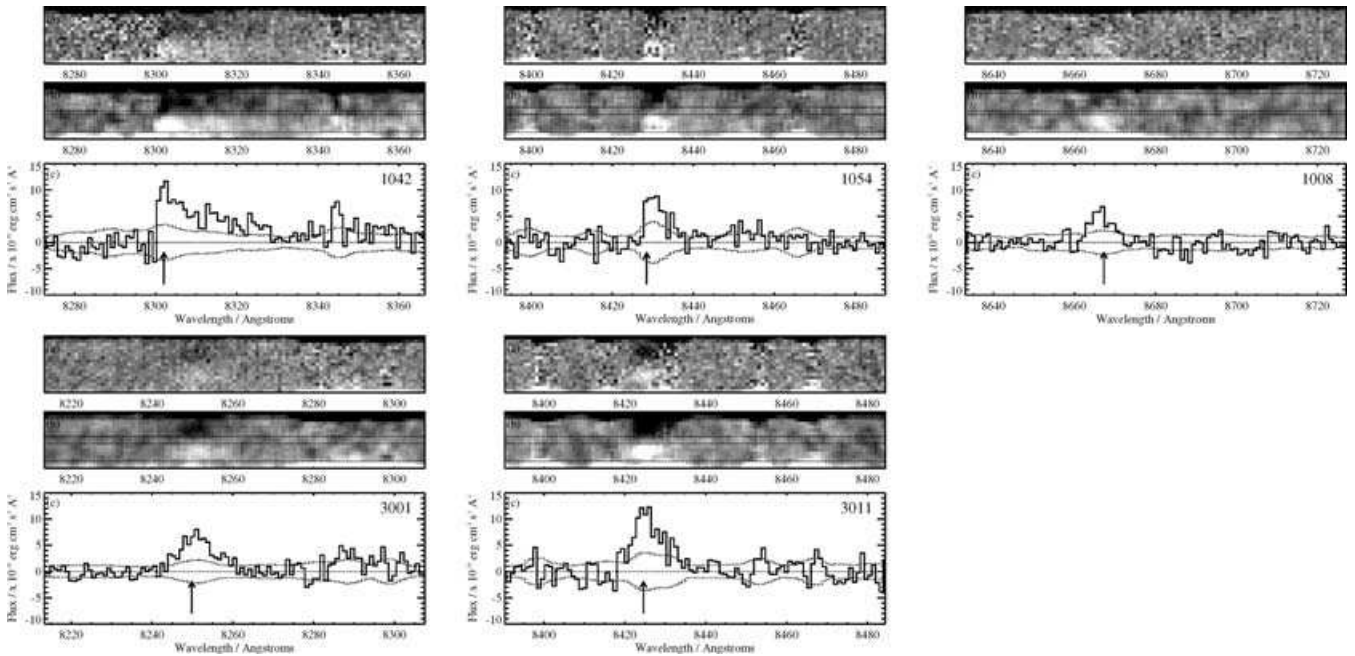


**Figure 2.** One- and two-dimensional spectra of the strong emission line candidates. The upper panel (a) shows the two-dimensional spectrum, the central panel (b) a spectrum smoothed over three pixels, and the lower panel (c) the one-dimensional combined spectrum extracted from both positive and negative channels. The source ID is shown on the right-hand side of panel (c) in each case. The $1\sigma$ s.d. in the background, smoothed over 15 Å and including the Poisson noise on the emission line flux is indicated with a dotted line. The arrow indicates the wavelength of the putative emission line.

are galaxies GDS J033235.79−274734.7 ($z = 1.223$) and GDS J033229.63−274511.3 ($z = 1.033$) from the ESO VLT/FORS2 survey of Vanzella et al. (2005). We detect the [O II] emission at $\lambda = 8285$ Å and 7577 Å, with line fluxes 1.53 and 1.52 $\times$ $10^{-17}$ erg cm$^{-2}$ s$^{-1}$, respectively.

For the Ly$\alpha$ detections, GLARE sources 1042 and 3001 were previously identified as line emitters in Paper I from the 2003 GLARE mask, Stanway et al. (2004b). GLARE 3011 was tentatively identified as a line emitter, and this identification is now strongly confirmed. GLARE 1054 and 1008 are presented for the first time here.

Since its discovery (SBM03#1 in Stanway et al. 2003) GLARE 1042 at $z = 5.83$ has been spectroscopically confirmed (Dickinson et al. 2004; Stanway et al. 2004a,b, – SiD002) and extensively studied, including in the infrared with *Spitzer* (Eyles et al. 2005; Yan et al. 2005, – #1ab). GLARE 1054 was identified from the $i'$-drop selection in the HUDF, GLARE 3001 and 3011 from the somewhat brighter GOODS selection. GLARE 1008 is a source selected from

the initial early data release list of red sources in the HUDF survey. It lies outside the final overlap region of the HUDF which has been used for catalogue construction and analysis, but within the noisy outer regions of the HUDF mosaic. It is technically below the detection limit of the GOODS survey, although it is faintly detected in the GOODS $z'$ band. It is faintly detected in the $z'$ band in the shallower edges of the HUDF.

Given the higher resolution and more sensitive flux limit of this spectroscopy, we can rule out a low-redshift interpretation for these sources and confirm them as $z \approx 6$ Ly$\alpha$ emitters. The spectral resolution of the GMOS configuration used in our 2004 GLARE mask is sufficient to resolve the [O II] $\lambda_{\mathrm{rest}} = 3727, 3729$ Å doublet (and does so in the case of the two known [O II] emitters on our 2004 GLARE mask), and we would expect to identify weaker emission lines such as [N II], [S II] within our observed redshift range if the detected line was H$\alpha$ ($\lambda_{\mathrm{rest}} = 6563$ Å). The other strong optical emission lines (H$\beta$ 4861, [O III] 4959, 5007) would always yield other strong lines

within our spectral range. Sources at these low redshifts are also unlikely to satisfy the colour cut criterion used for target selection.

All five detected strong Lyα emission lines also show significant asymmetry as expected for high-redshift emitters (in which the blue wing of the line is significantly self-absorbed, and the red wing broadened by re-emission). This phenomenon is well known at $z \approx 3$ and is believed to arise in outflows from the actively star-forming galaxies (Adelberger et al. 2003). Similar asymmetry has now been observed in all $z > 5.5$ galaxies confirmed to date by spectroscopy that resolves the Lyα emission line (e.g. Bunker et al. 2003), suggesting that similar outflows are produced at higher redshift galaxies.

### 3.2 Possible emission lines

We identify a further four sources (listed in Table 3) as possible line emitters. In most cases, the detection in each channel is of low significance, but the coincidence of positive and negative signals suggests that the emission lines are real. Alternately some candidate lines may lie on top of skylines, leading to the suspicion that these represent skyline residuals. These sources are illustrated in Fig. 3. All but one of the candidate emission lines lie shortward of the lower redshift limit selected by the $i'$-drop technique. Sources at these redshifts would be expected in a $v$-drop rather than $i'$-drop selection. It is possible for sources with large errors on their $i' - z'$ colour to scatter into the $i'$-drop selection, although it is unlikely that photometric scatter alone could explain this discrepancy.

Three of these sources were identified in the HUDF $i'$-drop sample, one (GLARE 3000) from the GOODS sample. GLARE 3000 was first identified as an $i'$-drop source in Stanway et al. (2003, SBM03#05) but considered likely to be an M or L class Galactic dwarf star, as it is unresolved in *Hubble Space Telescope* (*HST*) imaging. The candidate emission line in this source lies beside a strong sky line residual. FORS2 spectroscopy of this source by Vanzella et al. (2005) also interpreted the spectrum obtained as that of a Galactic star. The stellar identification is almost certainly correct, given the broadband colours and unresolved half light radius of this source, suggesting that possible emission lines at this significance should be considered highly suspect.

There are two possible emission lines of similar strength in GLARE 1067 (at 7037 and 7099 Å), rendering it unlikely that this source lies at high redshift. The observed line separation may be consistent with [O III] emission ($\lambda_{\rm rest} = 4959, 5007$ Å) at $z = 0.418$, although a galaxy at this redshift is predicted to have colours that are significantly bluer (i.e. $i' - z' < 0.5$ and detected in the $b$ band, as opposed to the observed $i' - z' = 1.4 \pm 0.2$ and no $b$ detection). In addition, the redward line of this [O III] doublet is expected to be three times stronger than the blueward line, while the observed emission peaks are of comparable strength. An alternate explanation might be

that two galaxies, separated by 3000 km s$^{-1}$ lie within the slit. While this source has a close neighbour (at $\alpha_{\rm J2000} = 03:32:35.8$, $\delta_{\rm J2000} = -27:48:49$, with a separation of $<1$ arcsec), the neighbouring galaxy is blue in colour ($i' - z' = 0.2$), and likely lies at significantly lower redshift. Therefore the most probable interpretation of these lines (if they are real) is that they represent [O III] emission arising not in the targeted galaxy but rather in the neighbouring source.

GLARE 1040 and GLARE 1086 are the most convincing candidates in this category. GLARE 1040, is an isolated source that clearly drops between the $i'$ and $z'$ bands, and is undetected in the HUDF $v$ band. The candidate emission line lies at $z = 5.2$, just shortward of the $i'$-drop selection, although it is possible for a faint galaxy such as this to scatter upwards into the selection window.

The candidate line in the final source, GLARE 1086, lies firmly in the redshift range selected by the $i'$-drop technique, and may well be a high-redshift emission line, although the detection is too weak to rule out a low redshift [O II] explanation, or to detect line asymmetry.

Finally, we identify signals in a further five sources as 'unlikely' emission lines. These are shown in Table 4 and Fig. 4. Although the dipole signal from the first two sources appears strong, they lie on bright skylines and so may be partly or wholly due to sky subtraction residuals. They may also arise as a result of charge diffusion from the adjacent slit. Both candidates lie at $\lambda > 10\,000$ Å (not far from the 10 500 Å Si bandgap) where the diffusion is strong. The signal in the remaining candidates is weak. Slit GLARE 6050 was a blank sky slit, and there is nothing visible in any waveband at the depth of the GOODS imaging of this region. The possible serendipitous line emitter is offset from the centre of the slit by approximately 0.2 arcsec to the north.

### 3.3 Sources with no line emission

The remaining 21 science targets on the slitmask showed no evidence for line emission in the wavelength range observed, $\lambda_{\rm obs} \approx 7800$–$10\,000$ Å (corresponding to $5.4 < z < 7.2$, with some slit to slit variation depending on slit location).

Of these, 11 formed part of our high priority $i'$-drop selection, with marginal targets (five sources) and sky slits (five slits) constituting the remainder. We discuss the implications of these non-detections of line emission below.

It is possible that, despite optimizing our experimental set-up for sky line subtraction, we are missing flux from emission lines that fall in regions dense with skylines. The noise in such areas is greater than the slit average, making identification of line candidates more difficult. Some 35 per cent of the wavelength coverage of this spectroscopy lies under sky lines (defined as regions where sky

**Table 3.** Possible line emitters on the 2004 GLARE mask. As in Table 2. The redshift assumes that the emission detected is the Lyα line at $\lambda_{\rm rest} = 1215.7$ Å.

| Slit | RA and Dec. J(2000) | Alternate ID | $z$ | $z'_{\rm AB}$ | $i' - z'$ | Line flux (erg cm$^{-2}$ s$^{-1}$) | $W^{\rm rest}_{\rm Ly\alpha}$ (Å) | $L_{\rm Ly\alpha}$ ($10^{42}$ erg s$^{-1}$) |
|---|---|---|---|---|---|---|---|---|
| 1040 | 03 32 38.28 −27 47 51.3 | 24458 | 5.21? | $27.51 \pm 0.07$ | $1.60 \pm 0.17$ | $0.17 \times 10^{-17}$ | 20.2 | 0.49 |
| 1067 | 03 32 35.83 −27 48 48.9 | 14210 | 4.84?[a] | $28.08 \pm 0.10$ | $1.43 \pm 0.24$ | $0.30 \times 10^{-17}$ | 81.5 | 0.72 |
| | | | 4.78?[a] | | | $0.31 \times 10^{-17}$ | 88.0 | 0.73 |
| 1086 | 03 32 30.14 −27 47 28.4 | 30359 | 6.10? | $28.13 \pm 0.11$ | $1.46 \pm 0.25$ | $0.37 \times 10^{-17}$ | 68.1 | 1.53 |
| 3000[b] | 03 32 38.80 −27 49 53.7 | | 5.08? | $25.65 \pm 0.03$ | $>3.50$ | $0.11 \times 10^{-17}$ | 2.24 | 0.30 |

[a]GLARE 1067 has two emission lines, which are consistent with [O III] at $z = 0.418$; if these are instead Lyα, both are at $z < 5$.
[b]GLARE 3000 is most likely a low-mass Galactic star.
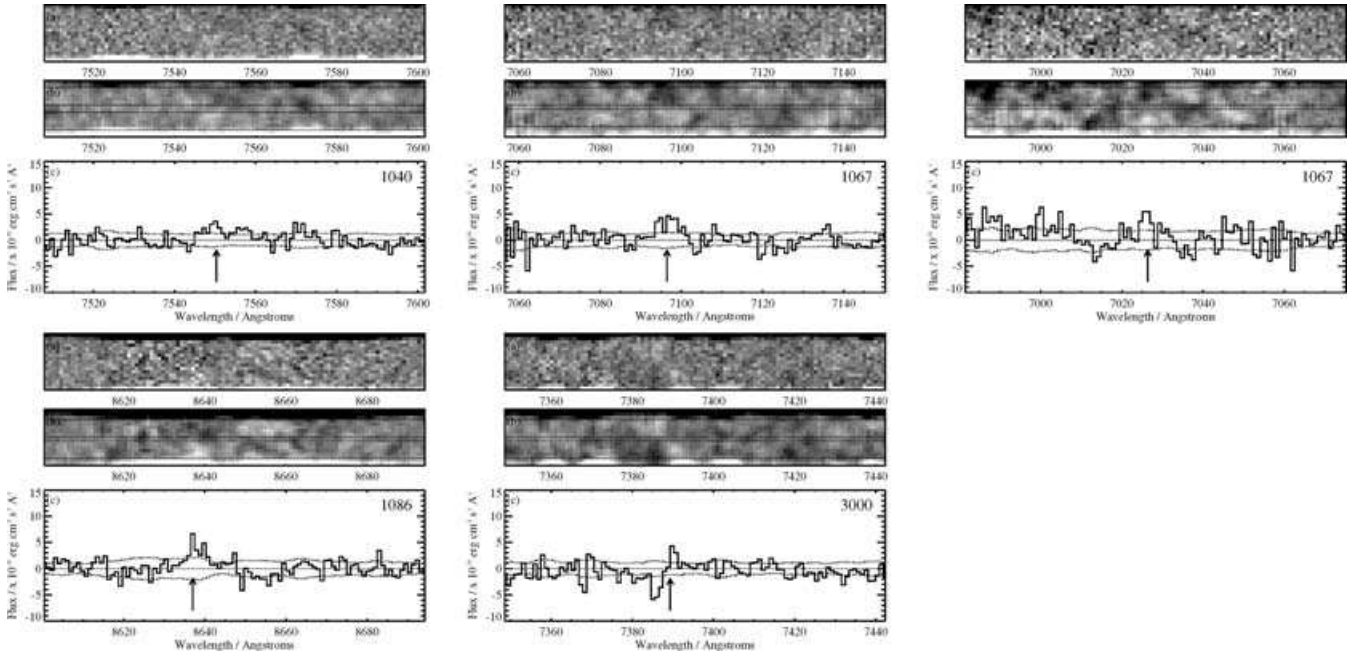
**Figure 3.** One-dimensional combined spectrum extracted from both channels of the image, and two-dimensional spectra, of the possible emission line candidates. Panel descriptions are as in Fig. 2.

**Table 4.** The five emission line candidates classified as 'unlikely' to be real. A limit has been placed on the possible serendipitous emitter GLARE 6050 based on non-detection in the $z'$ band to our imaging depth of $z'_{AB} = 28.5$. Column headings as in Table 2.

| Slit | RA and Dec. J(2000) | Alternate ID | $z$ | $z'_{AB}$ | $i' - z'$ | $W^{\rm rest}_{\rm Ly\alpha}$ (Å) |
|---|---|---|---|---|---|---|
| 1034 | 03 32 39.454 −27 45 43.42 | 52086 | 7.24? | $27.97 \pm 0.09$ | >2.43 | 10.6 |
| 1030 | 03 32 41.184 −27 49 14.81 | 10188 | 7.46? | $27.10 \pm 0.05$ | $2.04 \pm 0.16$ | 4.4 |
| 3015 | 03 32 27.910 −27 49 41.98 | | 5.67? | $27.30 \pm 0.10$ | >1.85 | 16.7 |
| 6050[a] | 03 32 37.450 −27 49 47.60 | | 7.05? | − | − | >104 |
| 8005 | 03 32 34.392 −27 45 33.01 | | 4.69? | $27.11 \pm 0.16$ | $1.15 \pm 0.36$ | 66.6 |

[a]6050 is a 'blank sky' slitlet.

emission exceeds 150 per cent of the interline sky continuum level) which leave Poisson noise and sky brightness fluctuation residuals of varying strength, although only 10 per cent lies under strong sky-lines (sky line emission >5 times sky continuum). The noise under the residuals of bright sky lines is a factor of 2.5 greater than that between lines, and might also be prone to systematics in the sky subtraction leading to potentially spurious emission lines.

Only half of LBGs at $z \approx 3$ show Ly$\alpha$ in emission (Shapley et al. 2003), and one quarter have $W^{\rm rest}_{\rm Ly\alpha} > 20$ Å. Given that we reach a limiting rest-frame equivalent width of $\leqslant 6$ Å for the majority of our targets, we might naïvely expect to observe emission in half our slits, less 10 per cent lost to strong sky line residuals. However, the fraction of LBGs with emission at $z \approx 6$ is still unknown, and it is likely that a large fraction of $z \approx 6$ $i'$-drop galaxies will not be spectroscopically confirmed until the continuum level is reached with either longer exposures or more sensitive telescopes, and interstellar absorption lines can be used for redshift determination (see e.g. Dow-Hygelund et al. 2005, for rest-frame UV continuum spectroscopy of a bright $z = 5.5$ galaxy).

Finally, in the case of the marginal candidates used to fill the slitmask, it is possible that the true redshift of the sources lies above

$z = 4.5$ (set by the dual requirements of non-detection in the $b$ band, and the $i' - z'$ colours of these sources), but below the limit of our spectroscopy. Two of the slits without detections were placed on $v$-drop galaxies expected to lie in this range, while a further four slits were placed on sources slightly too blue to meet our strict selection criteria. It seems unlikely that photometric scatter could place these sources in our detectable redshift range.

We will discuss the equivalent width limits on our $i'$-drop galaxies in Section 4.

### 3.4 Agreement with other spectroscopic surveys

A subset of sources in our sample have also been observed spectroscopically as part of the concerted campaign of follow-up observations to the GOODS survey.

Sources in the GOODS-S field have been targeted for 8-m spectroscopy by FORS 2 on the VLT (Vanzella et al. 2006), by DEIMOS on Keck (Stanway et al. 2004a; Bunker et al. 2006) and by GMOS on Gemini (Paper I and this work). In addition, this field was surveyed with the *HST*/ACS grism as part of the GRAPES survey (Malhotra et al. 2005). This slitless spectroscopy has been obtained to
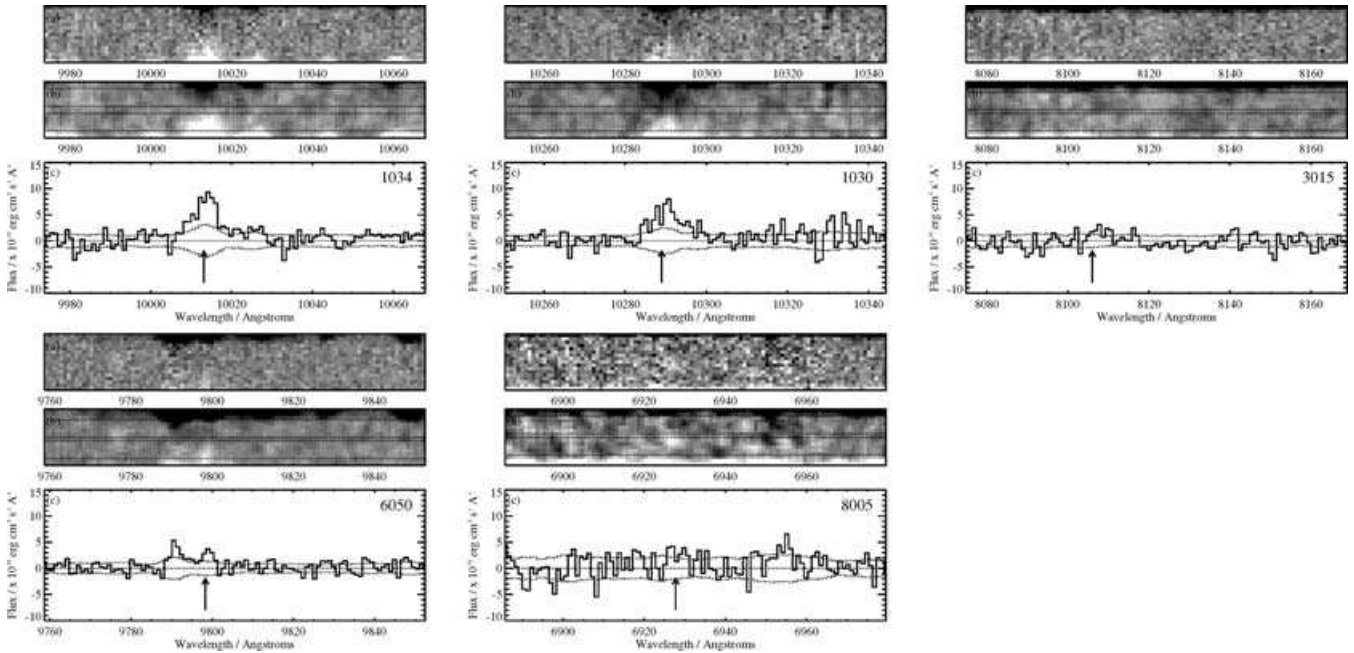
**Figure 4.** One- and two-dimensional spectra of the 'unlikely' emission line candidates presented in Table 4. Panel descriptions are as in Fig. 2.

varying depths, and at different spectral resolutions. In particular, the GRAPES grism spectroscopy is of too low a resolution to detect all but the highest equivalent width Lyα emission lines adjacent to the Lyα forest continuum break (cf. e.g. the DEIMOS spectrum of SBM03#1/GLARE1042 in Stanway et al. 2004a showing the strong Lyα line, with the *HST*/ACS spectrum of the same object, SiD002, in fig. 2a of Dickinson et al. (2004), which shows a continuum break but the line is washed out). However, GRAPES does provide a redshift estimate by localizing the wavelength of the Lyα break in the spectrum.

Where redshifts have been determined by multiple groups, our results are generally in reasonable agreement with previous observations, given the difficulty in obtaining precise redshifts from the self-absorbed and resonantly broadened Lyα lines at moderate spectral resolution. In the case of GLARE 1042, our measured redshift of $z = 5.83$ is in close agreement with that measured by FORS 2 ($z = 5.82$, Vanzella et al. 2005), by the GRAPES team ($z = 5.8$, Malhotra et al. 2005) and, using Keck/DEIMOS spectra, by Stanway et al. (2004a, $z = 5.83$). GLARE 3001 was spectroscopically identified by FORS 2 as a line emitter at $z = 5.78$, agreeing with our redshift of $z = 5.79$.

GLARE 1054 and 1030 were both placed at $z = 5.7$ by GRAPES spectroscopy (Malhotra et al. 2005). This contrasts with our measured redshifts of $z = 5.9$ for GLARE 1054 and (tentatively) $z = 7.4$ for GLARE 1030. The discrepancy for GLARE 1054 is within the expected level of agreement for GRAPES grism spectroscopy and so these results are consistent. Given the low significance of our line candidate in GLARE 1030, and the $i'$-drop redshift selection function, the GRAPES redshift remains the more likely.

The remaining source, GLARE 3000 was identified by the VLT/FORS 2 observations as a Galactic star on the basis of weakly detected [O I] and [N II] lines. This source, which corresponds to the unresolved candidate SBM03#5 in Stanway et al. (2003), falls in our 'possible' category. We note that the FORS II spectrum is flagged with their quality class 'C' and that there is no secure continuum detection. Despite this, a Galactic star is still the most likely

identification of this target, illustrating the caution with which we present our fainter line candidates.

No other target on our 2004 GLARE mask has been reported as a line emitter by other teams, or has an estimated redshift from GRAPES spectroscopy.

### 3.5 Limits on NV and other emission lines

LBGs at $z \approx 3$ show few other emission lines in the rest-frame ultraviolet. The composite spectrum of $\approx 1000$ such galaxies produced by Shapley et al. (2003) shows weak emission features due to Si II* ($\lambda_{\rm rest} = 1265, 1309, 1533$ Å), O III] ($\lambda = 1661, 1666$ Å) and C III] ($\lambda = 1908$ Å), and absorption features due to stellar winds, primarily Si II and C IV.

The presence of an AGN in our target galaxies could also lead to the presence of emission lines due to high excitation states, primarily NV ($\lambda_{\rm rest} = 1238.8, 1242.8$ Å) and Si IV ($\lambda = 1394, 1403$ Å), and rarely O V] ($\lambda = 1218$ Å).

For a galaxy at $z = 6$, our spectra extend to rest-frame wavelengths of $\approx 1428$ Å. Given that we are not able to measure a high S/N continuum on any one target, we are unable to measure absorption features in the spectra, and therefore confine ourselves to searching for evidence of other emission features in the spectra of our Lyα emitters.

A careful inspection of our five good Lyα emission line candidates does not provide evidence for any other emission lines at the redshift of Lyα. While this is not surprising given the weakness of secondary lines, the failure to detect NV in this spectroscopy suggests a large Lyα/NV ratio. Using our $3\sigma$ limit on undetected lines as an upper constraint on NV flux we determine that $f({\rm Ly}\,\alpha)/f({\rm NV}) > [10.5, 4.5, 2.8, 5.1, 7.5]$ ($3\sigma$), respectively, for GLARE targets [1042, 1054, 1008, 3001, 3011]. Typical line ratios for AGNs are $f({\rm Ly}\,\alpha)/f({\rm NV}) = 4.0$ (Osterbrock 1989), while those for galaxies are greater than this. The limits we determine disfavour an AGN origin to the Lyα flux in all but the faintest target (in which the constraint is too weak to make a firm statement). These limits

constrain AGN activity, if present, to only a weak contribution to the rest-frame ultraviolet flux.

## 4 THE EQUIVALENT WIDTH DISTRIBUTION OF GLARE LINE EMITTERS

### 4.1 The observed equivalent width distribution

Using the mean variance in the background of the exposed slits, and the broadband magnitudes of the targeted galaxies, we are able to calculate limits on the rest-frame equivalent width $W_0$ for those sources which satisfy our colour selection criteria and yet are undetected in our spectroscopy. These are presented in Table 5. In each case we assume that the galaxy lies at the mean $i'$-drop redshift ($z = 6.0$) and that the emission line has not been lost behind the subtraction residual of a bright night sky line.

Combining our line limits with those sources for which emission lines have been identified or tentatively proposed forms a sample of 24 sources uniformly selected from their $i'$-drop colours. The resultant distribution of Ly$\alpha$ equivalent widths is plotted in Fig. 5.

If all the sources for which candidate emission lines are identified in this paper prove to be $z \approx 6$ Ly$\alpha$ emitters, then the escape fraction of Ly$\alpha$ photons at $z \approx 6$ appears qualitatively similar to that at $z \approx 3$. From our $z \approx 6$ sample, 66 per cent of the sources (16 out of 24) have Ly$\alpha$ equivalent widths $<25$ Å, compared with 75 per cent at $z \approx 3$ (Shapley et al. 2003), although the lower redshift sample loses a smaller fraction due to skyline contamination. The samples probe to similar points on the luminosity function in both cases (approximately $0.1 L^*$). These fractions are consistent within the errors on our small number statistics. Harder to explain in comparison with lower redshift galaxies is the tail stretching to very high equivalent widths ($>200$ Å) observed in this survey, a trait also observed in some narrowband selected sources at this redshift (e.g. Malhotra & Rhoads 2002) and in other $i$-dropout LBGs (e.g. Dow-Hygelund et al. 2006, who find one source with $W_0 = 150$ Å). Although the number statistics are small, we observe four line emitters ($17 \pm 8$ per cent) with equivalent widths in the range 50–100 Å, and a further four with $W_0 > 100$ Å (three of which come from our 'robust' list of line emitters). This contrasts with the LBG population at $z \approx 3$ in which $<5$ per cent of galaxies have line emission with $W_0 > 100$ Å (Shapley et al. 2003).

While high-redshift galaxies at both redshifts are selected on their rest-frame ultraviolet continuum and the spectral break caused by Ly$\alpha$ absorption, the two populations are not identical.

The sample discussed here reaches some two magnitudes fainter than the tentatively proposed and still uncertain typical luminosity $L^*$ at $z \approx 6$ (Bunker et al. 2004; Bouwens et al. 2006). This contrasts with a sample reaching just one magnitude below $L^*$ at $z = 3$. Shapley et al. (2003) considered subsamples at $z = 3$, dividing their spectroscopic data into quartiles based on rest-frame equivalent width. They found a modest trend in the strength of line emission with magnitude. Galaxies in their highest equivalent width quartile are some 0.2 mag fainter on average than their quartile of weak to moderate line emission. It is possible that the strong line emission observed here is more typical of sources with faint rest-frame ultraviolet continuum suggesting that faint sources differ physically from brighter members of the population.

A second difference between the samples is intrinsic rather than arising from a selection effect. Several authors (e.g. Lehnert & Bremer 2003; Stanway et al. 2005; Bouwens et al. 2006) have now observed that LBGs at $z > 5$ have steeper rest-frame ultraviolet slopes than those at $z \approx 3$. Bouwens et al. (2006) interpret this as indicating that the dust properties of this population evolve over redshift. While a steep rest-ultraviolet slope can also arise due to low metallicity or a top-heavy IMF (as discussed below) dust evolution is a natural interpretation. At $z \approx 6$ the universe is less than 1-Gyr old and galaxies may not have had time to develop a high dust content. Shapley et al. (2003) found that $z \approx 3$ galaxies with high equivalent widths in Ly$\alpha$ also had lower mean dust extinction. Ly$\alpha$ photons are resonantly scattered by dust and hence the line is preferentially absorbed with respect to the rest-frame ultraviolet continuum. If the distribution of Ly$\alpha$ equivalent widths in the $z \approx 3$ population is truncated by dust absorption, this could produce an apparent 'excess' of strong lines at high redshift. However, even zero dust absorption cannot explain equivalent widths exceeding 200 Å unless the sources are also very young and very low in metallicity. The full explanation for the equivalent width distribution observed in the GLARE data may well be a combination of these effects and those discussed below.

Several other possible explanations exist for both the steepening of the rest-frame UV slope and the difference in equivalent width distributions. An interpretation of contaminant galaxies at lower redshifts seems unlikely due to our $i'$-drop selection criteria; low-redshift sources with strong spectral breaks are likely to have more than one emission line in our observed redshift range.

A high equivalent width line can arise if the observed Ly$\alpha$ photons excited by a population of AGNs rather than by young, hot stars. The luminosity function of AGNs is poorly constrained at these magnitudes and redshifts, but the space density of such sources is expected to be very low (e.g. the $z > 6$ Sloan Digital Sky Survey (SDSS) QSOs, Fan et al. 2003). At $z \approx 6$, the deep 2 Ms X-ray exposure of the UDF and surrounding region (Alexander et al. 2003)

**Table 5.** The 2004 GLARE targets for which no line emission was observed. Limits on the equivalent width are calculated using the $z'$-band magnitude to determine the continuum level, the $3\sigma$ s.d. in the background as the minimum line flux and accounting for IGM absorption, assuming the galaxy lies at $z = 6$. 'Alt' indicates an alternate ID in Bunker et al. (2004).

| ID | Alt | RA and Dec. | $z'_{AB}$ | $i' - z'$ | $W^{rest}_{Ly\alpha}$ (Å) |
|---|---|---|---|---|---|
| 1001 | 48989 | 03 32 41.43 −27 46 01.2 | $28.26 \pm 0.12$ | $>2.1$ ($2\sigma$) | $<6.5$ |
| 1004 | 46223 | 03 32 39.86 −27 46 19.1 | $28.03 \pm 0.10$ | $>2.37$ ($2\sigma$) | $<5.2$ |
| 1009 | 12988 | 03 32 38.50 −27 48 57.8 | $28.11 \pm 0.11$ | $>2.29$ ($2\sigma$) | $<5.6$ |
| 1045 | 21111 | 03 32 42.60 −27 48 08.8 | $28.02 \pm 0.11$ | $1.67 \pm 0.26$ | $<5.2$ |
| 1047 | 35271 | 03 32 38.79 −27 47 10.8 | $28.44 \pm 0.14$ | $1.33 \pm 0.30$ | $<7.6$ |
| 1060 | 11370 | 03 32 40.06 −27 49 07.5 | $28.13 \pm 0.11$ | $>2.28$ ($2\sigma$) | $<5.7$ |
| 1077 | 16258 | 03 32 36.44 −27 48 34.2 | $27.64 \pm 0.07$ | $1.42 \pm 0.16$ | $<3.7$ |
| 3002 | | 03 32 43.35 −27 49 20.4 | $26.89 \pm 0.07$ | $1.42 \pm 0.20$ | $<1.8$ |
| 3030 | | 03 32 48.94 −27 46 51.4 | $27.04 \pm 0.08$ | $1.41 \pm 0.23$ | $<2.1$ |
| 3033 | | 03 32 49.08 −27 46 27.7 | $27.18 \pm 0.09$ | $1.40 \pm 0.27$ | $<2.4$ |
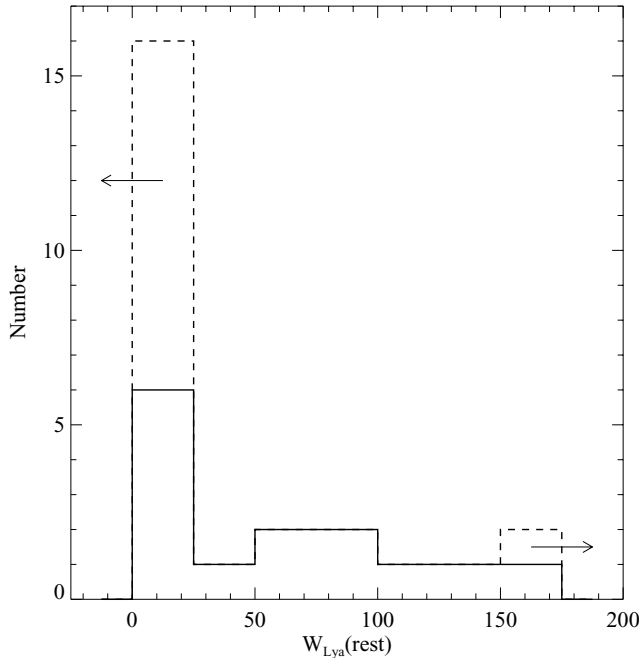
**Figure 5.** The distribution of rest-frame equivalent widths for the GLARE mask, divided into bins of 25 Å. Line emission candidates are shown with solid lines, sources with equivalent widths >150 Å are shown at 150 Å, and those for which only upper and lower limits are available are added to the distribution to produce the dotted lines.

would detect only the brightest AGN ($L > 10^{42}\,\mathrm{erg\,s^{-1}\,cm^{-2}}$). None of the GLARE targets are detected in this X-ray observation. AGNs would also be expected to show emission lines that are not just strong but also broad, while none of the GLARE line candidates are broad. There is also an absence of high-ionization lines such as NV 1240 Å which are common in AGNs.

The tail of line emitters extending to higher equivalent widths may also arise from a difference in the fundamental properties of the stellar population between $z \approx 6$ and that at lower redshifts.

Modelling of emission from metal-free Population III galaxies predicts rest-frame Lyα equivalent widths >1000 Å for young starbursts (<2 Myr), decreasing to $W(\mathrm{Ly}\alpha) \sim 500$ Å for older bursts (Schaerer 2002). These very high equivalent widths arise from the relatively hard spectrum of metal-free reactions in the most massive stars. However it is unlikely that zero metallicity (population III) stars are still contributing significantly to the emission from massive stars almost a billion years after the Big Bang, particularly given the identification of stellar populations >100 Myr old in some $z >$ 5 sources (e.g. Egami et al. 2005; Eyles et al. 2005). Further evidence for moderate metallicity at $z > 5$ has been observed in the spectroscopy of bright AGNs from the SDSS. Metals including iron (Barth et al. 2003) and carbon (Maiolino et al. 2005) have been detected from even the highest redshift quasar (at $z = 6.4$).

By contrast, even 1/20th solar metallicity leads to a sharp reduction in the peak (zero age) equivalent width predicted to ∼300 Å, with a more typical $W(\mathrm{Ly}\alpha) \sim 100$ Å by an age of 10–100 Myr (Malhotra & Rhoads 2002). Most of the candidate emission lines presented in this study can hence be explained with normal, if low metallicity, populations. However, at least two of our good line emission candidates have rest-frame equivalent widths exceeding 200 Å. This is possible if the galaxy is in the first few Myr of an ongoing

starburst, but may also provide evidence for variation in the IMF of star formation.

High equivalent widths of Lyα emission can arise from a 'top-heavy' IMF (i.e. star formation weighted towards a population of high-mass stars). Malhotra & Rhoads (2004) calculated the Lyα equivalent width expected for a metal-enriched population with a very extreme IMF, weighted towards massive stars (i.e. IMF slope $\alpha = 0.5$). As is the case for low metallicity populations, the flux is weighted towards a harder spectrum, and Lyα emission is strengthened. They found that such an IMF could explain line equivalent widths of up to 240 Å at ages of a few Myr, with higher IMFs possible for very young bursts.

The hard rest-frame ultraviolet spectrum associated with such an IMF may also be consistent with the steep rest-frame ultraviolet spectral slopes observed in $z \approx 6$ galaxies (e.g. Stanway et al. 2005). While the evidence from the GLARE study is limited, with the number of high equivalent width sources small, the existence of such sources suggests that the environment of star formation at $z \approx 6$ is less metal enhanced, or weighted towards more massive stars than that at $z \approx 3$.

### 4.2 Implications of high equivalent widths

The presence of a tail of large equivalent width emission line sources has implications for the redshift distribution expected from an $i'$-drop selection.

The redshift distribution and number densities of $i'$-drop galaxies have usually been calculated assuming a negligible contribution from line emission to the measured magnitudes and colours. In the case of line emitters with rest-frame equivalent widths $W_0 < 30$ Å this is a reasonable assumption, with the contribution to $z'$ flux amounting to a few per cent.

For line emitters with larger equivalent widths there can be a significant effect on the selection function of $i'$-drop galaxies. This effect falls into three main regimes as illustrated by Fig. 6. If the emission line falls in the $i'$-band filter (i.e. $z < 6.0$), then the $i' - z'$ colour of the galaxy is reduced by the line emission, and sources with high equivalent widths fall out of the colour-magnitude selection window. A source at our $z'$ detection limit with a rest-frame Lyα equivalent width of 100 Å can be as blue as $i' - z' = 0.67$ (AB) and an intrinsic line width of 150 Å would lead to a colour of just $i' - z' = 0.46$ (AB). These colours are similar to those of much lower redshift galaxies. Ensuring a complete selection of line emitting galaxies at $5.6 < z < 6.0$ is therefore impossible using a simple colour-selected sample without also including a great many lower redshift contaminant sources.

If the line emission falls in $z'$ filter, the $i' - z'$ colour is enhanced and galaxies with continuum flux below the $z'$ limit are promoted into the selection window. Hence at $z > 6.5$ the $i'$-drop criterion can select a population of low continuum, strong line emission sources rather than the continuum break sources it targets. There is also a redshift range in which the line emission would fall in the overlap region between filters and both effects compete.

This effect may lead to a bimodal redshift distribution for $i'$-drop galaxies, with weak emission line sources preferentially selected towards lower redshift, and high equivalent width sources selected at higher redshifts. It is necessary to quantify the equivalent width distribution, combining galaxies at the faint limits explored here with brighter galaxies, in order to tightly constrain the galaxy luminosity function at any given redshift.
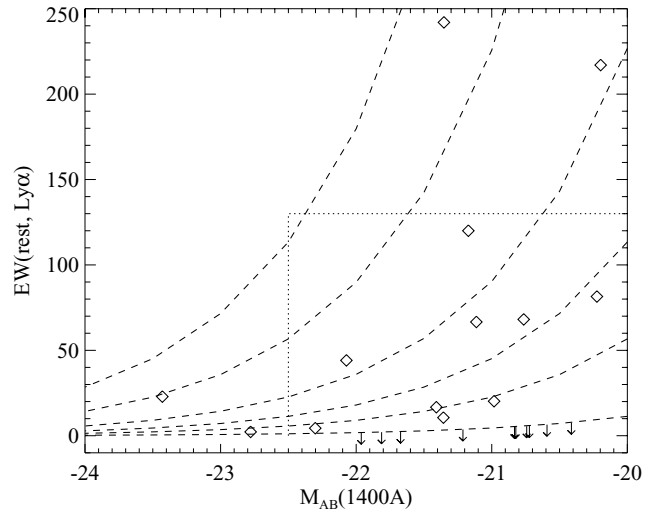
As Fig. 6 illustrates, our good line emission candidates all lie in regions of parameter space affected by equivalent width selection
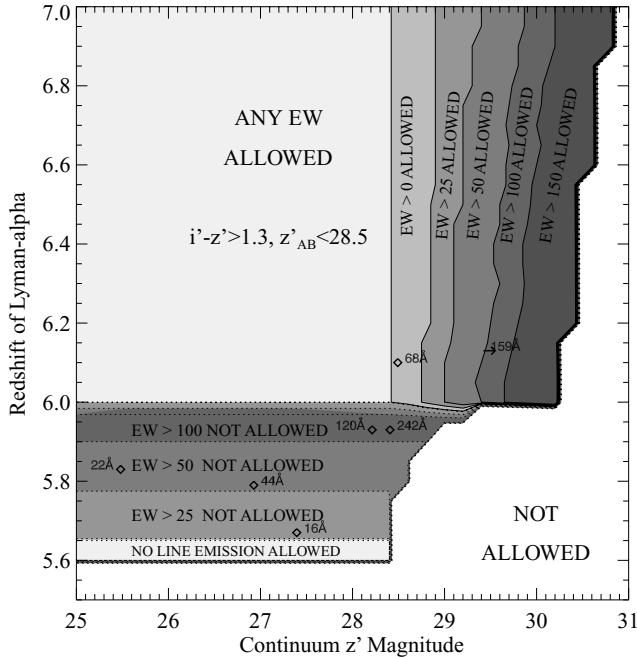
**Figure 6.** The effects of Lyα equivalent width on the *i*-drop selection function. Contours show the equivalent width line required to place a galaxy with the given redshift and continuum magnitude into the selection window. Solid lines indicate minimum equivalent width required, dotted lines indicate maximum equivalent width permitted. In the absence of line emission, all galaxies above the limiting observed magnitude and at $z > 5.6$ are detected. In the presence of strong line emission, galaxies at $z < 6.0$ fall out of the selection as the emission line lies in the *i'* band, while fainter galaxies at high redshift can be promoted into the selection due to brightening of the measured *z'* magnitude. The properties of the seven *i'*-drop sources with redshifts in this range are shown with diamonds.



**Figure 7.** The equivalent width distribution of GLARE line emitters as a function of absolute magnitude. The region of parameter space surveyed by the compilation of Ando et al. (2006) is bordered by a dotted line. Dashed lines indicate the loci $z = 6$ emission lines with luminosities of $10^{44}, 5 \times 10^{43}, 2 \times 10^{43}, 10^{43}, 5 \times 10^{42}$ and $10^{42}$ erg s$^{-1}$ (from top left-hand side to bottom right-hand side). Our equivalent width limit for sources without line detection corresponds to a rest-frame luminosity of $10^{42}$ erg s$^{-1}$, assuming those sources lie at $z \approx 6$.

biases. Our candidates lie in parameter space theoretically allowed for their equivalent width with two exceptions – GLARE 1054 and 3011 both have strong emission lines in the tail of the *i'* filter that should have forced their $i' - z'$ colours out of our selection function. We note, however, that that both of these sources have $i' - z'$ colours within 1σ of our minimum selection cut-off, and may have scattered up into out selection. Only one source is boosted into the selection function by virtue of its line emission rather than continuum flux, suggesting that our sample is, as expected, dominated by continuum-selected sources. If we are indeed missing sources with high emission line equivalent widths at the low-redshift end of our survey (where our redshift selection function is at its peak), then our conclusion that the distribution of line emission at high redshift extends to larger equivalent widths is strengthened.

This effect has interesting implications for the luminosity functions presented in the literature for $z \approx 6$ galaxies. If the *i'*-drop criteria are overestimating the number density of faint continuum sources (due to contamination by a tail in the distribution of strong line emitters) then it is possible that the faint end slope of the luminosity function is shallower than hitherto reported. If there is a large number of strong emitters at $5.6 < z < 6.0$ that have fallen out of the colour selection, then the number density of sources at these redshifts could be underreported. This may contribute towards the discrepancy between the observed evolution in the LBG luminosity function between $z = 4$ and $z \approx 6$ (e.g. Bunker et al. 2004; Bouwens et al. 2006) and the reported lack of evolution in the Lyα emitter

luminosity function over the same redshift range (e.g. Malhotra & Rhoads 2004).

Ando et al. (2006) studied the equivalent width distribution of a heterogeneous sample of *i'*-drop and narrowband selected galaxies with spectroscopically confirmed Lyα emission at $z \approx 6$. They commented on an apparent dearth of UV-luminous galaxies with strong Lyα emission lines, noting an increase in the fraction of strong line emitters at $M_{AB} = -21$. In Fig. 7 we show the equivalent distribution of the GLARE line emitters as a function of absolute magnitude.

We detect five bright sources with a line luminosity brighter than $2 \times 10^{43}$ erg s$^{-1}$, thus occupying a regime unoccupied by the Ando et al., sample. Of these, two possible emission line sources have equivalent widths greater than any in the previous sample. The four sources with a calculated line luminosity between $5 \times 10^{43}$ and $10^{44}$ erg s$^{-1}$ are uniformly distributed in absolute magnitude.

Although the number statistics of our sample is small, our sample is uniformly selected by broadband magnitude, removing possible biases due to the combination of two methods. Narrow-band surveys are biased towards sources with faint continuum and bright Lyα emission lines, whereas the *i'*-drop selection method is more uniformly sensitive to Lyα emission except at the very faint and low-redshift ends of the sample. Our results do not support those of Ando et al., although clearly further observations are required to clarify the fraction of line emitters at bright magnitudes. It is possible that the fraction of sources with high equivalent width line emission is subject to environmental effects (e.g. the local number density of galaxies). The small HUDF field is, of course, subject to the effects of cosmic variance (Bunker et al. 2004). For sources as clustered as LBGs at moderate redshifts are known to be, a variance in number density of 40 per cent is expected in a field this size (Somerville et al. 2004).
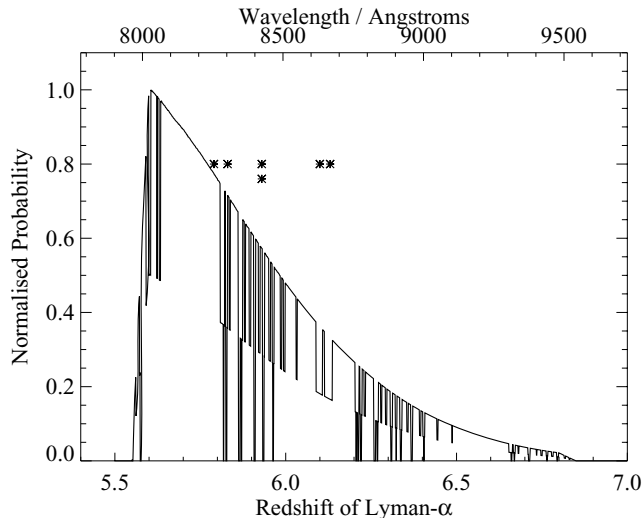
**Figure 8.** The redshift distribution expected for sources with line detection in the GLARE spectroscopy. Assumed a distribution of magnitudes given by a Schecter luminosity function, with constant number density over the redshift interval $5.5 < z < 7.0$, modified by the sensitivity of Gemini/GMOS in our configuration, and assuming that a line is undetected if under a skyline, and has a 50 per cent probability of being detected if under a weaker skyline. The redshifts of our candidate line emitters are shown by asterisks, see Section 5.1 for details.

# 5 DISCUSSION

## 5.1 The redshift distribution of *i'*-drop galaxies

The redshift distribution expected for line emitters detected by the GLARE survey is the convolution of the selection functions imposed by the *i'*-drop selection criteria and by the spectral response of Gemini/GMOS in this configuration, modified by the probability of detecting a line that falls on a night sky emission line.

In Fig. 8 we show the expected distribution of emission line redshifts, neglecting the influence of strong line emission on source magnitude and colour (see above), and assuming a Schecter (1976) luminosity function with parameters $L^* = L^*(z=3)$, $\alpha = -1.9$ and $\phi^* = \phi^*(z=3)$ (Stanway 2004). Changing the parameters of the luminosity function has a slight effect on the shape of the distribution, with a reduction in $L^*$ with increasing redshift slightly broadening the peak of the distribution in redshift space.

We take the conservative assumption that a source has a detection probability of 0 per cent if lying on a very strong line ($>5\times$ the interline sky continuum) and 50 per cent on top of a weaker sky line ($>1.5\times$ sky continuum level). The night sky spectrum is measured directly from our spectroscopy.

Clearly, our survey is most sensitive to sources lying towards the lower redshift end of our redshift range, and to sources lying in the low OH line regions commonly exploited by Lyα surveys at $z \approx$ 5.7 and $z \approx 6.6$. None the less, we have a reasonable probability of detecting sources in the skyline complexes at $z < 6.5$, particularly if the source emission lies between skylines.

Given this theoretical sensitivity distribution, it is interesting to note that the five robust line emitters presented in this paper (and one possible emission line also lying in this redshift range) do not fall at the peak of the detection sensitivity distribution, but rather within the skyline complexes. In Stanway et al. (2004b) we suggested weak evidence for large scale structure in the HUDF field at $z = 5.8$, based on the three redshifts known at the time. More recently Pirzkal et al.

(2004) have found evidence for an overdensity at $z = 5.9 \pm 0.2$ in the same field based on GRAPES Grism spectroscopy. Given that it unlikely that our fainter targets will yield redshifts with the current generation of spectrograph, confirmation of this may prove challenging. However, our results so far appear consistent with large scale structure at $z \approx 5.8$ in this field.

## 5.2 The space density of Lyα emitters

We have identified a total of 12 (five of which were strong) candidate emission lines with a luminosity in the range $(1 - 50) \times 10^{42}$ erg s$^{-1}$ in our sample of 24 *i'*-drop galaxy candidates. If this is indicative of the *i'*-drop selected galaxy population as a whole, and if the equivalent width distribution is invariant with magnitude, we would expect to observe line emission of this strength in approximately 25 (11 strong) of the 51 *i'*-drop galaxies identified in the HUDF by Bunker et al. (2004) (which were used by GLARE for candidate selection). Hence, this suggests a line emitter space density of 6.7 (2.9) $\times 10^{-4}$ ($\Delta \log L)^{-1}$ Mpc$^{-3}$), using the effective comoving volume for the *i'*-drop selection in the HUDF survey of $2.6 \times 10^4$ Mpc$^3$. This space density comparable to the space density of $6.3 \times 10^{-4}$ ($\Delta \log L)^{-1}$ Mpc$^{-3}$ estimated by Shimasaku et al. (2006) for Lyα emitters of comparable luminosity [(3–25) $\times 10^{42}$] at $z \approx 5.7$ in the *Subaru* Deep Field.

Similarly, at $z = 5.7$ the Lyman-Alpha Large Area Survey (LALA) found a number density of $3.2 \times 10^{-4}$ Mpc$^{-3}$ for Lyα emitters with $L > 10^{42}$ erg s$^{-1}$ (Malhotra & Rhoads 2004). This would predict the detection of 7 Lyα emitters to our detection limit in our survey volume. This is consistent with, although slightly lower, than the number of emitters we detect.

Inferring the space density of emitters from the relatively small sample in this survey is, of course, subject to large errors due to Poisson noise on the small number statistics. However, at least two physical explanations are possible for a discrepancy between the line emitter density found by GLARE and by LAE surveys. As mentioned in Section 5.1, the HUDF is in a region with a known overdensity of sources at $5.7 < z < 5.9$. GLARE is also likely to detect a higher apparent density of line emitters if the Lyα photon escape fraction is higher in the relatively faint galaxies studied here than in more massive galaxies. If this is true then the number of sources observed at faint magnitudes exceeds the number predicted from brighter surveys. This phenomenon may well be expected if the deeper potential well of more massive galaxies traps more dust and a denser ISM than that existing in the shallow potential wells of small, faint galaxies.

## 5.3 The emission line properties of sub-*L*$^*$ galaxies

This spectroscopy is the longest integrated exposure on a single mask using an 8m telescope. It reaches the faintest line limits available for a large sample with a homogeneous *i'*-drop colour cut. The $3\sigma$ limit in most slits is approx $4.1 \times 10^{-19}$ erg cm$^{-2}$ s$^{-1}$ Å$^{-1}$.

Hence we are able to observe line emissions from candidates significantly fainter than other surveys targeting *i'*-drop galaxies.

Given the expenditure in telescope resources required to reach these faint limits, it is likely that many of the HUDF candidates may well remain inaccessible to ground based spectroscopy until the advent of the Extremely Large Telescopes, and from space by JWST with NIRSpec. HUDF *i'*-drops can be identified with reasonable confidence to $z'_{AB} < 28.5$ (Bunker et al. 2004). A source with $z'_{AB} = 28.5$ and an emission line of $W = 20$ Å (rest) at $z = 6$, with complete Lyα absorption shortward of the line, would have a

contamination fraction of 13.5 per cent to the $z'$ band from this line, and a continuum flux of $6.4 \times 10^{-21}$ erg cm$^{-2}$ s$^{-1}$ Å$^{-1}$ – that is, a continuum flux a factor of ~10 less than we are able to detect at the $1\sigma$ level per spectral resolution element (6.5 Å). However, such a source would possess a line flux of $6 \times 10^{-18}$ erg cm$^{-2}$ s$^{-1}$, well within our detection limits for emission lines.

Hence, although emission lines are detectable in surveys such as this, even for the faintest of our target sources, continuum spectra will remain inaccessible for some time to come. Even GLARE 1042, the brightest $z \approx 6$ in the HUDF does not have sufficient S/N to in this spectroscopy to detect absorption features, even though the continuum is now detected at high significance. The detection of stellar absorption lines would provide valuable kinematic information on the galaxies and their outflows, however while such investigations may be possible on a stacked image of our faint spectra, it is impossible on individual slits. A stack of the faint GLARE spectra will be considered in a future paper.

## 6 CONCLUSIONS

In this paper we have presented spectroscopy of the faintest known sample of $i'$-drop galaxies, derived from the HUDF. An exposure of 36 h per target was obtained with the Gemini-South telescope.

Our main conclusions can be summarized as follows.

(i) We have obtained extremely deep spectroscopy for 29 science targets, reaching $3\sigma$ line flux limits of $2.5 \times 10^{-18}$ erg cm$^{-2}$ s$^{-1}$ – corresponding to equivalent width limits of $<6$ Å for the majority of our targets.

(ii) We identify five $i'$-drop galaxies as good Ly$\alpha$ emitter candidates, four as possible candidates, and a further five tentative emission lines which we consider unlikely to be real.

(iii) We have considered the observed equivalent width distribution of $i'$-drop galaxies in the HUDF, and identify a tail of line emitters with very high equivalent widths which is not seen in the lower redshift LBGs at $z \approx 3 - 4$.

(iv) Several possible explanations for this effect exist. These include a tendency towards stronger line emission in faint sources, extreme youth or low metallicity in the Lyman-break population at high redshift, or possibly a top-heavy IMF.

(v) At the low-redshift end of our selection function ($5.6 < z < 6.0$), the $i'$-drop selection method will fail to select line emitters with high equivalent width due to line contamination producing blue colours. In contrast, at the high-redshift end ($z > 6$), continuum-faint line emitters may enter the selection function if the Ly$\alpha$ line is sufficiently luminous. This has implications for the redshift and continuum magnitude selection function of $i'$-drop galaxies.

(vi) This sample significantly increases the number of faint $i'$-drop galaxies with known redshifts, and may begin to bridge the divide between continuum and line-selected galaxies at $z \approx 6$.

## REFERENCES

Abraham R. G. et al., 2004, AJ, 127, 2455
Adelberger K. L., Steidel C. C., Shapley A. E., Pettini M., 2003, ApJ, 584, 45
Alexander D. M. et al., 2003, AJ, 126, 539
Ando M., Ohta K., Iwata I., Akiyama M., Aoki K., Tamura N., 2006, ApJ, 645, L9
Barth A. J., Martini P., Nelson C. H., Ho L. C., 2003, ApJ, 594, L95
Becker R. H. et al., 2001, AJ, 122, 2850
Beckwith S. V. W. et al., 2006, AJ, 132, 1729,
Bouwens R. J. et al., 2004, ApJ, 606, L25
Bouwens R. J., Illingworth G. D., Blakeslee J. P., Franx M., 2006, ApJ, 653, 53
Bunker A. J., Stanway E. R., Ellis R. S., McMahon R. G., McCarthy P. J., 2003, MNRAS, 342, L47
Bunker A. J., Stanway E. R., Ellis R. S., McMahon R. G., 2004, MNRAS, 355, 374
Bunker A. J., Stanway E. R., Ellis R., McMahon R. G., Eyles L., Lacy M., 2006, New Astron. Rev., 50, 94
Dickinson M. et al., 2004, ApJ, 600, L99
Dow-Hygelund C. C. et al., 2005, ApJ, 630, L137
Dow-Hygelund C. C. et al., 2006, preprint (astro-ph/0612454)
Egami E. et al., 2005, ApJ, 618, L5
Eyles L. P., Bunker A. J., Stanway E. R., Lacy M., Ellis R. S., Doherty M., 2005, MNRAS, 364, 443
Fan X. et al., 2003, AJ, 125, 1649
Glazebrook K., Bland-Hawthorn J., 2001, PASP, 113, 197
Hook I. et al., 2003, SPIE, 4841, 1645
Lehnert M. D., Bremer M., 2003, ApJ, 593, 630
Maiolino R. et al., 2005, A&A, 440, L51
Malhotra S., Rhoads J. E., 2002, ApJ, 565, L71
Malhotra S., Rhoads J. E., 2004, ApJ, 617, L5
Malhotra S. et al., 2005, ApJ, 626, 666
Osterbrock D. E., 1989, Astrophysics of Gaseous Nebulae and Active Galactic Nuclei. Univ. Science Books, Mill Valley CA
Pirzkal N. et al., 2004, ApJS, 154, 501
Schaerer D., 2002, A&A, 382, 28
Shapley A. E., Steidel C. C., Pettini M., Adelberger K. L., 2003, ApJ, 588, 65
Shimasaku K. et al., 2006, PASJ, 58, 313
Somerville R., et al., 2004, ApJ, L121
Stanway E. R., 2004, PhD thesis, Univ. Cambridge
Stanway E. R., Bunker A. J., McMahon R. G., 2003, MNRAS, 342, 439
Stanway E. R., Bunker A. J., McMahon R. G., Ellis R. S., Treu T., McCarthy P. J., 2004a, ApJ, 607, 704
Stanway E. R. et al., 2004b, ApJ, 604, L13
Stanway E. R., McMahon R. G., Bunker A. J., 2005, MNRAS, 359, 1184
Steidel C. C., Pettini M., Hamilton D., 1995, AJ, 110, 2519
Steidel C. C., Adelberger K. L., Shapley A. E., Pettini M., Dickinson M., Giavalisco M., 2003, ApJ, 592, 728
Thompson R. I. et al., 2005, AJ, 130, 1
Vanzella E. et al., 2005, A&A, 434, 53
Vanzella E. et al., 2006, A&A, 454, 423
Yan H. et al., 2005, ApJ, 634, 109

This paper has been typeset from a T$_{\rm E}$X/L$^{\rm A}$T$_{\rm E}$X file prepared by the author.